Expanded View Figures

A

1	GGGCGAGGAGCTGTTCACCG
2	GAGCTGGACGGCGACGTAAA
3	GAAGTTCGAGGGCGACACCC
4	GGAGCGCACCATCTTCTTCA
5	GGCCACAAGTTCAGCGTGTC
6	GATGCCGTTCTTCTGCTTGT
7	GGTGGTGCAGATGAACTTCA
8	GGGCACGGGCAGCTTGCCGG

B

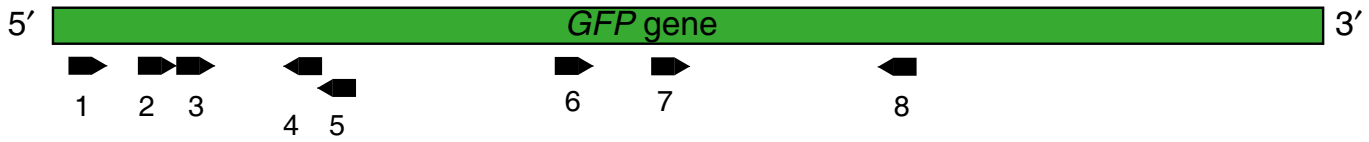

C

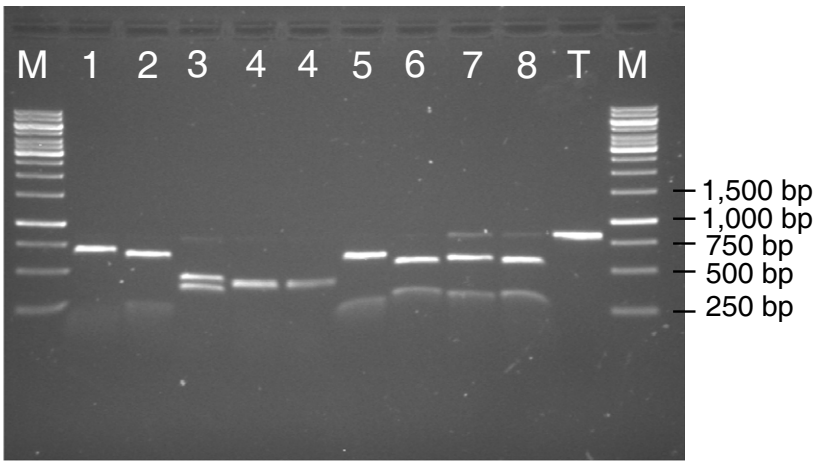

D

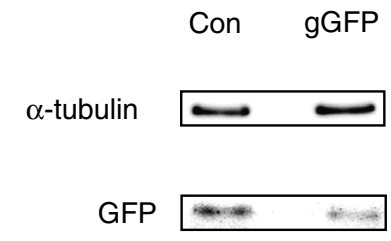

E

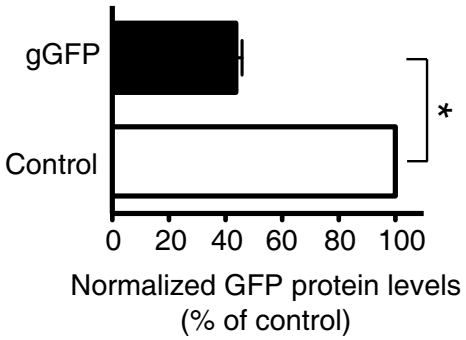

Figure EV1.

◀ **Figure EV1. Determination of the on-target Cas9 cutting efficiency directed by various gGFPs *in vitro* and of the disruption of GFP expression by the most appropriate gGFP *in vivo*.**

A Sequences of the tested gRNAs targeting *GFP*

B Orientation and location of the targeting sites of the gRNAs 1–8 described in (A) (black arrows) within the *GFP* gene (green bar).

C Agarose gel showing the effects of the gRNAs 1–8 described in (A) to direct Cas9-mediated cutting of an 800-bp-long *GFP* PCR product (lanes 1–8). T, template-only control with no gRNA added; M, DNA size marker. As the targeting site of the gRNA-1 was the one located most 5′ within the *GFP* gene, which increases the probability of obtaining disruption of gene expression, and the full-size template was virtually undetectable upon the *in vitro* reaction with Cas9 and this gRNA, it was selected for all *in vivo* experiments and is referred to as gGFP.

D, E Neocortex of mouse E13.5 embryos was *in utero* electroporated with a plasmid encoding Cas9_T2A_PaprikaRFP and gRNA targeting either *LacZ* (Con) or *GFP* (gGFP) as in Fig 1I, followed at E14.5 by FACS isolation of PaprikaRFP-positive cells and immunoblot analysis. (D) Representative immunoblots for α-tubulin (top), verifying the analysis of equal amounts of total protein, and for GFP, showing its reduced levels upon Cas9/gGFP plasmid electroporation. (E) Quantification of the GFP protein level, normalized to α-tubulin, 24 h after control (Con, white) or gGFP (black) Cas9 plasmid electroporation. Data are expressed as percentage of the respective control value (set to 100%) and are the mean of three immunoblots (six and eight embryos per condition, respectively, from three litters; gGFP 44%). Error bars indicate SEM; $*P < 0.05$ (Mann–Whitney *U*-test).

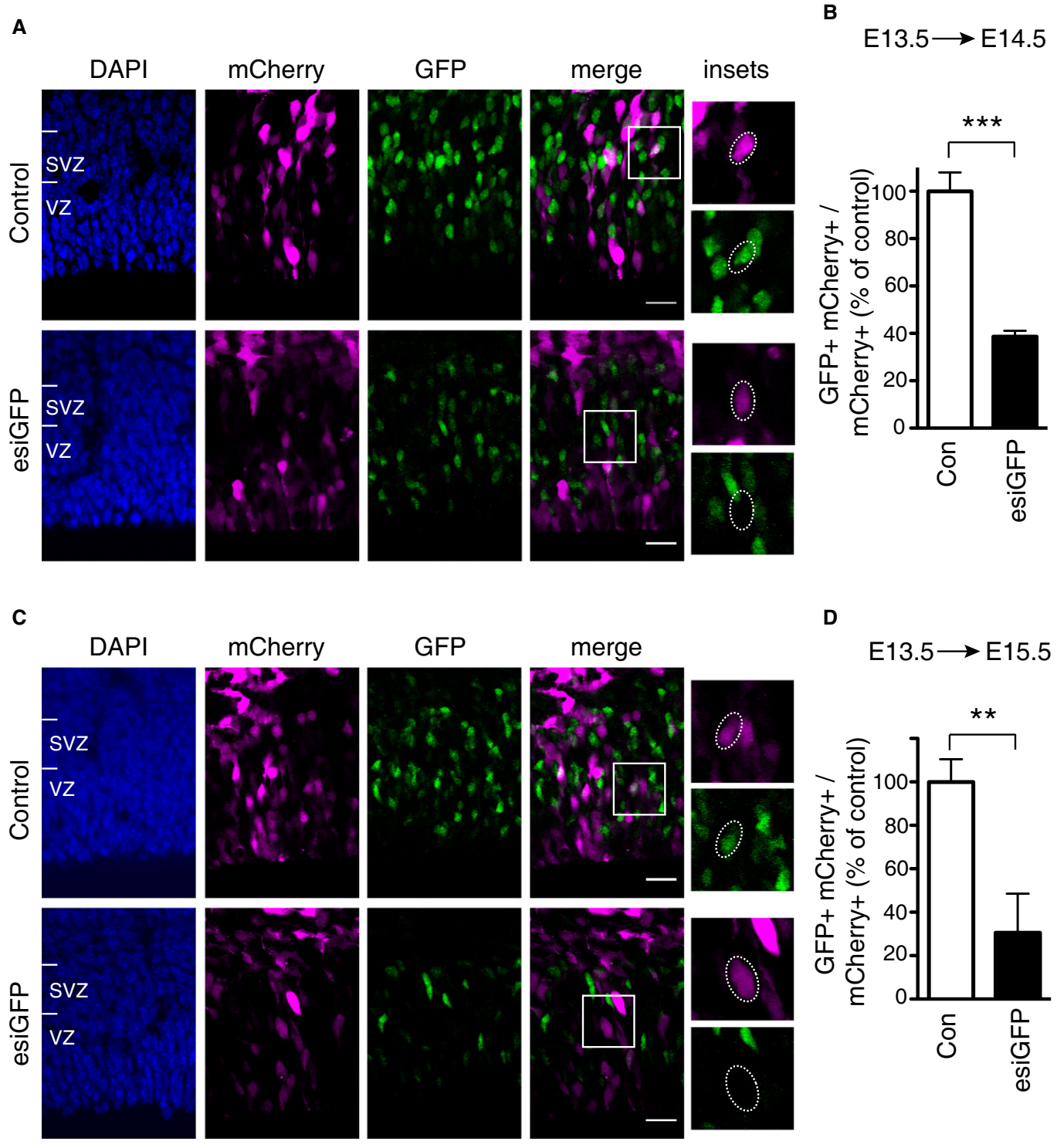

Figure EV2.

Figure EV2. RNAi-induced disruption of GFP expression in the neocortex of *Tis21*::GFP mouse embryos upon *in utero* electroporation.
Neocortex of mouse E13.5 *Tis21*::GFP embryos was *in utero* electroporated with esiRNAs targeting either luciferase (Control, Con) or GFP (esiGFP), followed by analysis at E14.5 (A, B) or E15.5 (C, D).

A VZ and SVZ of the electroporated areas showing targeted cells as revealed by mCherry fluorescence (magenta) and the effects of either control esiRNAs (top) or esiGFP (bottom) on GFP expression (green) 24 h after electroporation; blue, DAPI staining. Boxes indicate areas shown at higher magnification in the insets (35 × 35 μm). Dotted lines indicate nuclei of progeny of electroporated aRGCs; note the presence of GFP fluorescence in the control (top) and its absence upon esiGFP electroporation (bottom).

B Quantification of the proportion of mCherry-positive cells in the VZ plus SVZ that are GFP positive 24 h after control (Con, white) or esiGFP (black) electroporation. Data are the mean of three independent experiments (five embryos per condition in total, from three litters).

C VZ and SVZ of the electroporated areas showing targeted cells as revealed by mCherry fluorescence (magenta) and the effects of either control esiRNAs (top) or esiGFP (bottom) on GFP expression (green) 48 h after electroporation; blue, DAPI staining. Boxes indicate areas shown at higher magnification in the insets (35 × 35 μm). Dotted lines indicate nuclei of progeny of electroporated aRGCs; note the presence of GFP fluorescence in the control (top) and its absence upon esiGFP electroporation (bottom).

D Quantification of the proportion of mCherry-positive cells in the VZ plus SVZ that are GFP positive 48 h after control (Con, white) or esiGFP (black) electroporation. Data are the mean of three independent experiments (three embryos per condition in total, from three litters).

Data information: Controls were set to 100% (B, D) and the esiGFP conditions expressed relative to control (B, 39%; D, 30%). Error bars indicate SD; $^{**}P < 0.01$; $^{***}P < 0.001$ (Student's *t*-test). Scale bars, 20 μm. (A, C) All images are single optical sections.

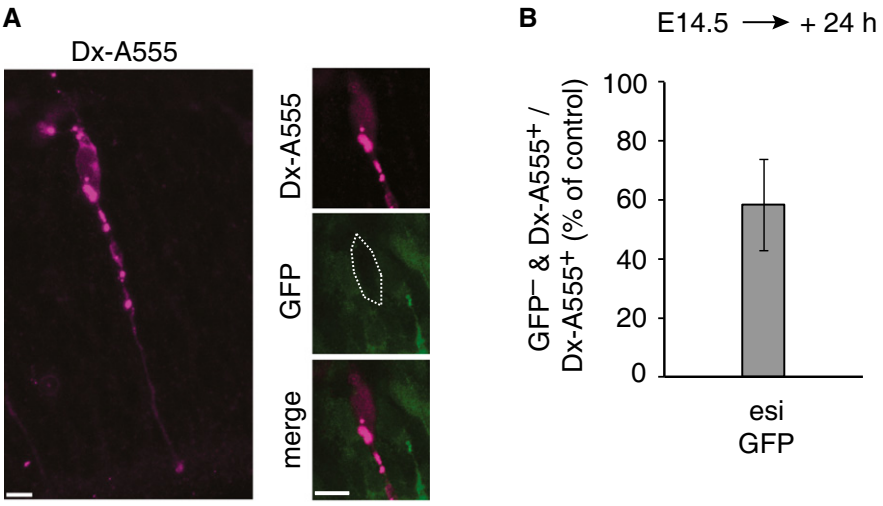

Figure EV3. RNAi-induced disruption of GFP expression in the daughter cells of single microinjected aRGCs in organotypic slices of telencephalon of *Tis21*::GFP mouse embryos.
Single aRGCs in neocortex in organotypic slices of telencephalon of mouse E14.5 *Tis21*::GFP embryos were microinjected with esiRNAs targeting either luciferase (control) or GFP (esiGFP) together with dextran 10,000-Alexa 555 (Dx-A555), followed by analysis after 24 h of culture.

A Maximum intensity projection (left, stack of 5 optical sections) of a daughter cell of a single aRGC microinjected with esiGFP (as revealed by Dx-A555 immunofluorescence, magenta), and a single optical section (right) of the cell body (dotted line) of that cell, showing an example of the lack of *Tis21*::GFP expression (as revealed by GFP immunofluorescence, green). Scale bars, 5 μm.

B Quantification of the proportion of Dx-A555$^+$ cells that lack *Tis21*::GFP expression (GFP$^-$) 24 h after esiGFP microinjection. Data are expressed as percentage of the value obtained 24 h after control esiRNA microinjection, which corresponded to that of dextran-only microinjected aRGCs [12], and are the mean of two independent experiments (21 and 23 Dx-A555$^+$ daughter cells of esiGFP-microinjected aRGCs scored, respectively); bar indicates the variation of the two individual values from the mean.

A

gTbr2-1: GGTGAGCTCGGTGAACCTGCCCGG

gTbr2-2: GGTTGTCTAAGTCCAGCCTCTGGGG

gTbr2-3: GGCGTCACTGAGCATGGCCGCGGGG

gTbr2-4: GGGGCAGCATGGAGCCGTAGGGG

B

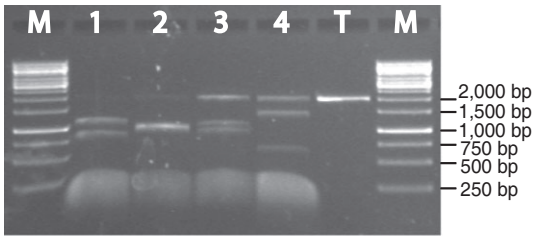

C

Name	Sequence	Strand	Locus
OT1	5′-GTGGCTTGGGAACCTGCCTGG-3′	sense	Chr X: 140,460,521-140,406,541
OT2	3′-GTGATCTCTGAACCTGCCTGG-5′	antisense	Chr X: 121,296,746-121,296,766
OT3	5′-GTGGCTCCGGAACCTGCCTGG-3′	sense	Chr 7: 16,078,668-16,078,688
OT4	3′-GTGAGATTAGTGAACCTGCCGGG-5′	antisense	Chr 1: 177,299,751-177,299,773

D

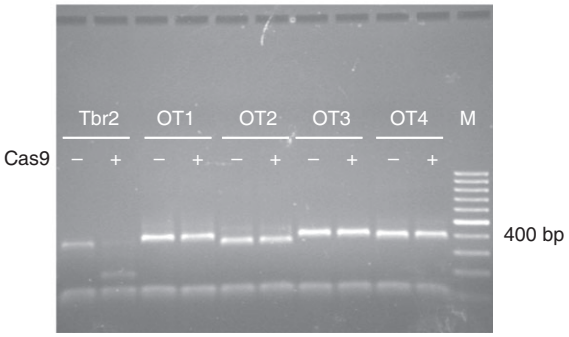

E

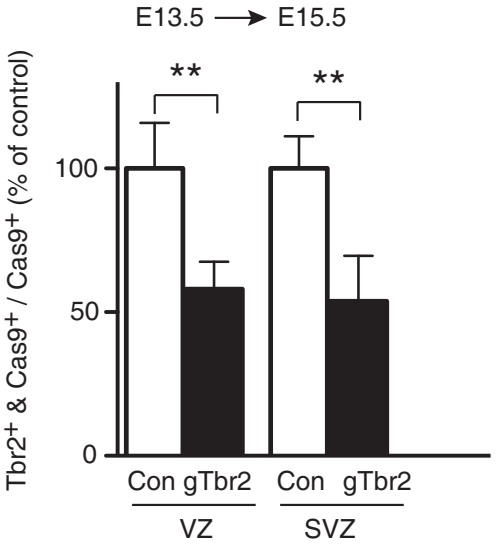

Figure EV4.

Figure EV4. Determination of the on-target Cas9 cutting efficiency and specificity when directed by various gTbr2s *in vitro*, and of the *in vivo* disruption of Tbr2 expression in the VZ and SVZ by the most appropriate gTbr2.

A, B *In vitro* assay of on-target Cas9 cutting efficiency directed by various gTbr2s. (A) Sequences of the 4 tested gRNAs targeting *Tbr2*, referred to as gTbr2-1 to gTbr2-4, all of which target exon 1. PAM (protospacer adjacent motif) is underlined. (B) Agarose gel showing the effect of the gTbr2-1 to gTbr2-4 described in (A) to direct Cas9-mediated cutting of a 2-kb-long *Tbr2* PCR product (lanes 1–4). T, template-only control with no gTbr2 added; M, DNA size marker. The predicted size of the PCR product fragments after Cas9/gTbr2-mediated cutting was as follows: gTbr2-1 (850 bp + 1,150 bp), gTbr2-2 (1,000 bp + 1,000 bp), gTbr2-3 (1,100 bp + 900 bp) and gTbr2_4 (1,400 bp + 600 bp). Note that the size of the fragments observed matched the predictions. As the targeting site of the gTbr2-1 was the one located most 5′ within exon 1 of the *Tbr2* gene, and as this gTbr2 exhibited the highest efficiency to direct Cas9-mediated cutting as assessed by the lack of detectable full-size template, it was selected for all *in vivo* experiments and for simplicity is referred to just as gTbr2.

C, D *In vitro* assay of the specificity of Cas9 cutting when directed by gTbr2. (C) Names, sequences, strands and genomic loci of the four major off-target sites (labelled OT1–4) of the gTbr2. (D) Agarose gel showing the lack of effect of gTbr2 to direct Cas9-mediated cutting of the ≈400-bp PCR products of the off-target loci (lanes OT1–OT4) as compared to that of the on-target locus (lane Tbr2). M, DNA size marker.

E CRISPR/Cas9-mediated reduction in Tbr2 immunoreactivity in both VZ and SVZ. Neocortex of mouse E13.5 embryos was *in utero* electroporated with a plasmid encoding Cas9_T2A_PaprikaRFP and either control gRNA (Con) or gTbr2, and analysed at E15.5 as in Fig 3A–D. Quantification of the proportion of $Cas9^+$ cells that are $Tbr2^+$ in the VZ (left) and SVZ (right) 48 h after control (Con, white) or gTbr2 (black) Cas9 plasmid electroporation. Data are the mean of four independent experiments (four embryos per condition, from four litters). Controls were set to 100% and the gTbr2 condition expressed relative to control (VZ, 58%; SVZ, 54%). Error bars indicate SD; $^{**}P < 0.01$ (Student's *t*-test).

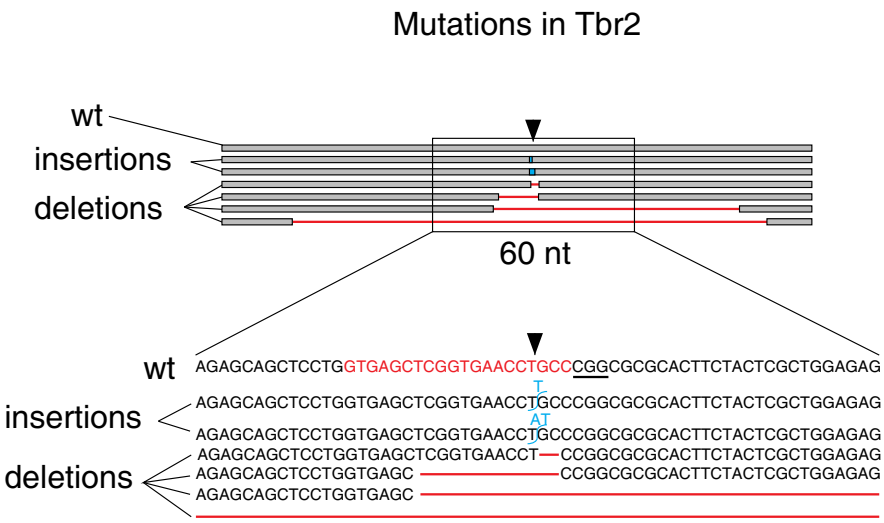

Figure EV5. Examples of types of indels caused by electroporation of Cas9/gTbr2 plasmid.
Illustration of the genomic locus 100 bp upstream and downstream (top) of the gTbr2 target site (indicated by black arrowheads) in the 5′ region of exon 1 of the *Tbr2* gene, showing the wild-type read (wt) and six examples of mutated reads with indels (two insertions: blue; four deletions: red). Bottom: the region 30 bp upstream and downstream of the target site (rectangle, 60 nt). gTbr2 targeting sequence is labelled in red in the wild-type sequence. Underlined nucleotides indicate PAM.